Future Motion Control to be Realized by In-wheel Motored Electric Vehicle

Peng He[1], Yoichi Hori[1]
[1]Department of Electrical Engineering
The University of Tokyo
4-6-1 Komaba, Meguro
Tokyo153-8505, Japan
ka@horilab.iis.u-tokyo.ac.jp
hori@iis.u-tokyo.ac.jp

Makoto Kamachi[2], Kevin Walters[2], Hiroaki Yoshida[2]
[2]Electronics Engineering Department
Mitsubishi Motors Corporation
Hashime-cho, Okazaki
Aichi Pref.,444-8501, Japan
makoto.kamachi@mitsubishi-motors.com
kevin.walters@mitsubishi-motors.com
hiroaki.yoshida@mitsubishi-motors.com

Abstract— **This paper discusses novel motion control strategies for in-wheel motored electric vehicle (EV), including 2-DOF control, dynamic optimal traction force distribution control and direct yaw moment control (DYC). Two electric vehicles, "UOT March II" and "COLT EV", are used for experiments. The control algorithms are verified by simulations and experiments, which show that the control strategies are efficient and effective.**

I. Introduction

In recent years, considering environmental protection and energy conservation, researches for EV have been put forward greatly. In the middle of the 21st century, EV will be the major tool of transportation system.

Due to the improvement of motor design and control technology, modern configurations are developed for EV. One of the latest configurations are motorized wheels, which mean motors are fitted into driving wheels of EV[1].

For vehicle chassis control, those configurations bring much more advantages. Electric motor can generate driving torque quickly and accurately. Also, motor torque can be measured and controlled independently[2]. Hence, not only conventional control methods can be easily implemented, but also some advanced control strategies can be realized, especially in severe driving situations. Based on these advantageous control methods, motored EV can be controlled as precisely as a robot.

In this paper, we propose two control strategies and verify them by experiments. Two EVs, which are "UOT March II"(The University of Tokyo) and "COLT EV" (Mitsubishi Motors Corporation) are used for experiments.

II. UOT March II

"UOT March II" is a novel motored vehicle, which can be used to realize some advanced control strategies. It was built in 2001 by remodeling Nissan March (shown in Fig.1). The most remarkable feature of this EV is that one motor is fitted into each wheel. And these four motors can be controlled independently. Fig.2 shows the motors for rear wheels.

Fig. 1. The EV named "UOT March II"

The specifications of "UOT March II" are shown in TABLE I.

TABLE I
The Specifications of "UOT March II"

Dimensions (L×W×H)		3695×1660×1525 (mm)
Weight		1100kg
Inertia moment		3.76×10^3 kgm^2
Tire Radius		0.26m
Motor (/unit)	Max. output	36kW
	Max. torque	77Nm
	Max. speed	8700rpm
	reduction gear	ratio 5.0
Battery	Type	Panasonic EC-EV1238
	Capacity	38Ah
	Voltage	12V × 19 modules

III. Linear analysis model of "UOT March II"

Linear vehicle model is used to express the dynamics of "UOT March II". The model is shown in Fig.3. δ is the steering angle. We assume that only the front wheel can be steered and the steering angles of both front wheels are equal to each other. V is the velocity vector of center

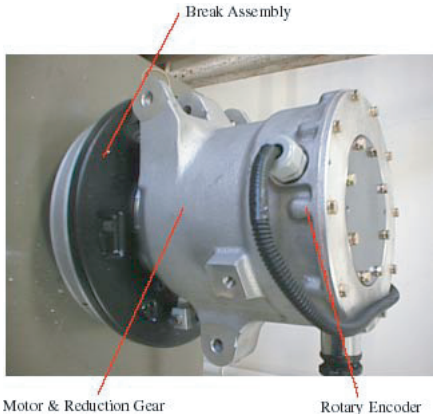

Fig. 2. In wheel motor for rear wheel

of gravity. β represents sideslip angle. γ represents yaw rate. M_z is the controlled yaw moment. For lateral motion control, β and γ are controlled state variables. The state equation is given by

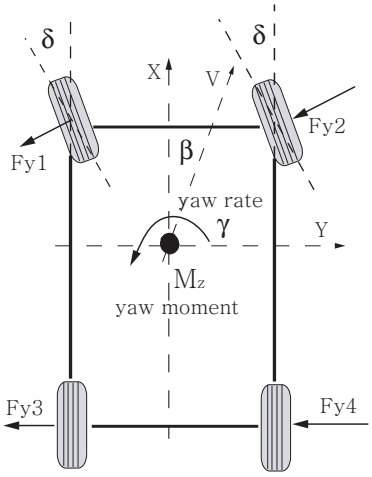

Fig. 3. Linear vehicle model for dynamic analysis

$$\begin{pmatrix}\dot{\beta}\\ \dot{\gamma}\end{pmatrix} = \underbrace{\begin{bmatrix}a_{11} & a_{12}\\ a_{21} & a_{22}\end{bmatrix}}_{A}\begin{pmatrix}\beta\\ \gamma\end{pmatrix} + \underbrace{\begin{bmatrix}b_{11} & b_{12}\\ b_{21} & b_{22}\end{bmatrix}}_{B}\begin{pmatrix}\delta\\ M_z\end{pmatrix} \quad (1)$$

where

$$\begin{aligned} A &= \begin{bmatrix} -\frac{2(C_f+C_r)}{MV} & -1-\frac{2(l_fC_f-l_rC_r)}{MV^2} \\ -\frac{2(l_fC_f-l_rC_r)}{I_z} & -\frac{2(l_f^2C_f+l_r^2C_r)}{I_zV} \end{bmatrix} \\ B &= \begin{bmatrix} \frac{2C_f}{MV} & 0 \\ \frac{2l_fC_f}{I_z} & \frac{1}{I_z} \end{bmatrix} \end{aligned} \quad (2)$$

M is the vehicle mass, I_z is the inertia moment, C_f (C_r) is the cornering stiffness of front (rear) tire.

IV. Yaw rate stability control strategy

In order to improve maneuverability of "UOT March II", we propose a control strategy, which is shown in Fig.4. It is a kind of integrated control method. In this strategy, force feedforward control and state feedback control are used. Further, dynamic optimal traction force distribution control is used.

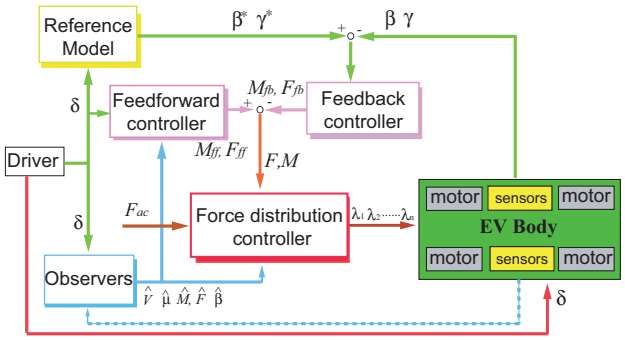

Fig. 4. 2-DOF control integrated with dynamic optimal traction force distribution used for EV motion control

The control objective is to make the EV to follow the desired yaw rate value while keeping its side slip angle minimum. Force feedforward control and state feedback control are integrated with each other to form 2-DOF control.

V. 2-DOF control

A. Reference model

According to Eq.1, the relationship between yaw rate γ and steering angle δ is determined as follows.

$$\frac{\gamma^*(s)}{\delta(s)} = \frac{k_R}{1+\tau_R s} \quad (3)$$

where, k_R and τ_R are the steady state gain and the time delay constant of yaw rate response.

B. Feedforward control

The feedforward control law is designed as[3]

$$M_{ff}(s) = G_{ff}\delta_f(s) \quad (4)$$

where G_{ff} is the proportional gain of the feedforward controller. $M_{ff}(s)$ is the controlled yaw moment. $\delta_f(s)$ is the steering angle.

G_{ff} can be given by Eq.5,

$$G_{ff} = \frac{b_{11}a_{22} - a_{12}b_{21}}{a_{12}b_{22}} \quad (5)$$

where the parameters are defined in Eq.1.

C. Feedback control

Feedback controller is designed as a *LQG* regulator. The state variables to be controlled are γ and β. The *LQG* regulator is designed as follows

$$\begin{aligned} &\min_{M_{fb}} \int_0^\infty ((x-x^*)^T Q_1 (x-x^*) \\ &+(M_{fb}-M_{fb}^*)^T R_1 (M_{fb}-M_{fb}^*))dt \quad (6)\\ &M_{fb} = K_{fb}x \quad (7)\\ &x = (\gamma, \beta)^T \quad (8) \end{aligned}$$

where x is the state variables. x^* is the reference value. Weight matrices Q_1 and R_1 are determined by experiments. M_{fb} is the controlled yaw moment. K_{fb} is given by the resolution of Ricatti equation.

VI. Dynamic optimal traction force distribution

As Fig.4 shows, the inputs of the distribution controller are yaw moment and driving force. In this paper, driving force is assumed to be zero, and only the force commands for four motors are given. We need to calculate the force commands by less number of inputs. Therefore, there is a redundancy problem. An optimal sequential quadratic programming (SQP) method is used to resolve that redundancy and to realize dynamic optimal traction force distribution control[4][5].

If four tires are all in adhesion state, yaw moment M_z can be given by Eq.9

$$M_z(t) = \left(-\frac{d_f}{2}, \quad \frac{d_f}{2}, \quad -\frac{d_r}{2}, \quad \frac{d_r}{2}\right) \cdot \left(F_{fl}(t), \quad F_{fr}(t), \quad F_{rl}(t), \quad F_{rr}(t)\right)^T \tag{9}$$

where d_f and d_r are front and rear tread. $F_{fl}(t)$ and $F_{fr}(t)$ are front left and front right traction force. $F_{rl}(t)$ and $F_{rr}(t)$ are rear left and rear right traction force.

Since traction force can be a function of longitudinal tire slip ratio, Eq.9 can be expressed as

$$M_z(t) = \left(-\frac{d_f}{2}, \quad \frac{d_f}{2}, \quad -\frac{d_r}{2}, \quad \frac{d_r}{2}\right) \cdot \left(f(\lambda_{fl}(t)), \quad f(\lambda_{fr}(t)), \quad f(\lambda_{rl}(t)), \quad f(\lambda_{rr}(t))\right)^T \tag{10}$$

Eq.10 can be expressed as

$$M_z(t) = D \cdot f(\lambda(t))^T \tag{11}$$

where $f(\lambda(t)) = (f(\lambda_{fl}(t)), f(\lambda_{fr}(t)), f(\lambda_{rl}(t)), f(\lambda_{rr}(t)))$. D=$(-\frac{d_f}{2}, \frac{d_f}{2}, -\frac{d_r}{2}, \frac{d_r}{2})$, $\lambda_{fl}(t)$ and $\lambda_{fr}(t)$ are front left and front right tire ratio. $\lambda_{rl}(t)$ and $\lambda_{rr}(t)$ are rear left and rear right tire ratio.

According to Eq.11, $\lambda(t)$ can be given by dynamic inverse mapping

$$\lambda(t) = Q(M_z(t), \lambda(t-T), M_z(t-T), ..., \lambda(t-kT), M_z(t-kT), ...) \tag{12}$$

where Q is a special function. T is the sampling time. $\lambda(t)$=$(\lambda_{fl}(t), \lambda_{fr}(t), \lambda_{rl}(t), \lambda_{rr}(t))$.

SQP method is used to resolve Eq.12 and calculate the optimal slip ratio for every tire by Eq.13[5].

$$\min_{\lambda(t)} ||W_1(\lambda(t) - \lambda_d)||_2 + ||W_2(\lambda(t) - \lambda(t-T))||_2 \tag{13}$$

subject to Eq.9.

where, λ_d is the desired optimal slip ratio which is determined by road condition estimation. W_1, W_2 are weight matrices which are determined by experiments.

Resolving Eq.13, the dynamic inverse mapping (as Eq.12 shows) can be obtained as

$$\lambda(t) = \tau_u \lambda(t-T) + \tau_v M_z(t) \tag{14}$$

Eq.14 is the dynamic optimal traction force distribution control law that we use, where τ_u is the time delay coefficient and τ_v is the proportional coefficient, which are determined by experiments.

VII. Simulation results

Simulations are performed to verify the proposed algorithm. In the beginning of simulation, the velocity of vehicle is 60 km/h and friction force coefficient is 0.8. The desired slip angle is equal to zero. The total driving force is also assumed to be zero. At the time of 2s, steering angle is changed to realize "J-turn" motion.

As Fig.5 shows, when the vehicle is controlled by 2-DOF control law but without optimal traction force distribution control, it could not follow the desired yaw rate quickly and accurately. The slip angle of vehicle body is big. It might cause instability for EV handling.

On the contrary, when 2-DOF control integrated with optimal traction force distribution control, the results show that the vehicle could show a quick response and follow the desired yaw rate quite well. It also could keep the slip angle of vehicle body smaller. It means maneuverability of EV is improved. Lateral forces which can be disturbance for handling is suppressed.

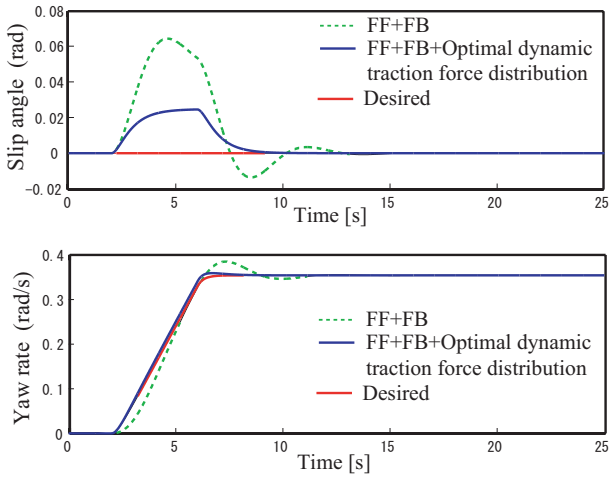

Fig. 5. Simulation results

VIII. COLT EV

Mitsubishi Motors Corporation (MMC) has started research and development for next generation electric vehicles - in-wheel motor base platform for pure electric vehicle, hybrid electric vehicle, and fuel cell vehicle - under the MIEV (Mitsubishi In-wheel motor Electric Vehicle) concept. In this paper COLT EV prototype, a pure electric vehicle, is chosen as our test vehicle. Investigation of DYC's effect based on experiments, especially with the objective to improve vehicle handling and stability is discussed.

A description of the system configuration for the COLT EV is given below. It is made from the mass produced COLT by (i) removing the engine, transmission and fuel

tank, (ii) installing an inverter box under the luggage compartment, traction battery to the position of the fuel tank, and in-wheel motors to each rear wheel, which is shown in Fig.6. The specification is shown in TABLE II.

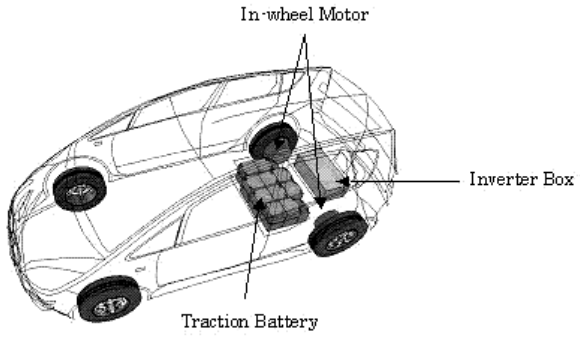

Fig. 6. Parts Layout of COLT EV

TABLE II
COLT EV Specifications

Dimensions (L×W×H)		3885×1680×1550 (mm)
Curb weight		1150kg (F:467kg/R:683kg)
Max. speed		150km/h (93mile/h)
Tire		185/55R15
Motor (/unit)	Max. output	20kW
	Max. torque	100Nm
	Max. speed	9000rpm
	Internal reduction gear	Planetary gear, ratio 6.0
Battery	Type	Lithium-ion
	Capacity	40Ah
	Voltage	14.8V × 22 modules

IX. Identification of vehicle model

To construct the DYC logic it is necessary to understand the relations between (i) steering-angle and the vehicle dynamics and (ii) motor torque difference and the vehicle dynamics. Through experiment we will identify the transfer functions from steering-angle to yaw rate and from motor torque difference to yaw rate respectively.

A. Linear model

From linear approximation using the simple bicycle model Eq.1, the transfer functions from steering angle θ and motor torque difference $T_{\rm dif}$ to yaw rate γ are defined as follows:

$$\begin{aligned}\gamma &= \frac{A_G(1+T_G s)}{1+\frac{2\zeta}{\omega_n}s+\frac{1}{\omega_n^2}s^2}\theta + \frac{A_H(1+T_H s)}{1+\frac{2\zeta}{\omega_n}s+\frac{1}{\omega_n^2}s^2}T_{\rm dif} \quad (15)\\ &= G(s)\theta + H(s)T_{\rm dif}\end{aligned}$$

Here, A_G and A_H are steady gains, T_G and T_H are lead time constants, ζ is damping coefficient, ω_n is natural frequency of yaw rate.

B. Identification experiment

[Method for Steering Angle Input]
Impose steering angle pulse input while driving at constant speed (80km/h). Pulse width is set approximately 0.5s and pulse peak value is limited to produce about 0.4G lateral acceleration. This is commonly used as the vehicle dynamics test method[6].

[Method for Motor Torque Difference Input]
Impose pulse shape motor torque difference while driving at constant speed (80km/h) and with steering angle fixed at 0 position. Pulse width is set at 0.5s and its peak set at the largest possible value.

[Results]
Vehicle response to steering angle change is shown in Fig.7 (top is steering angle, middle is yaw rate and bottom is lateral acceleration). Data of motor torque difference input is similar (figure omitted).

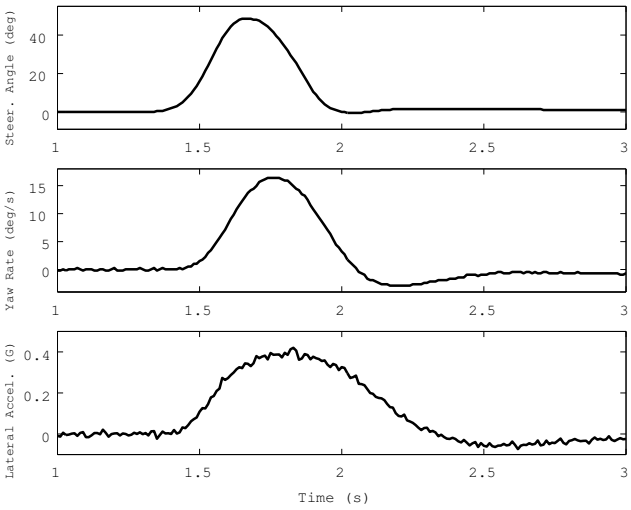

Fig. 7. Experimental Data of Steering Angle Input

C. Calculation

[Method]
Discrete Fourier Transformation is performed on the input (steering angle or motor torque difference) and output (yaw rate), then frequency response is calculated from this output/input ratio. Finally through curve-fitting method the transfer functions $G(s)$ and $H(s)$ are approximated. Considering Eq.15 the numerators are set to first order whereas the denominators are set to second order and common to $G(s)$, $H(s)$.

[Results]
Bode diagram of the calculated results is shown in Fig.8. Here, solid line shows fitted curve for transfer function $G(s)$, and dashed line is for transfer function $H(s)$. The identified parameters correspondent to Eq.15 are as follows: $\omega_n = 8.91$, $\zeta = 0.665$, $A_G = 0.382$, $T_G = 0.0880$, $A_H = 0.0418$, $T_H = 0.109$.

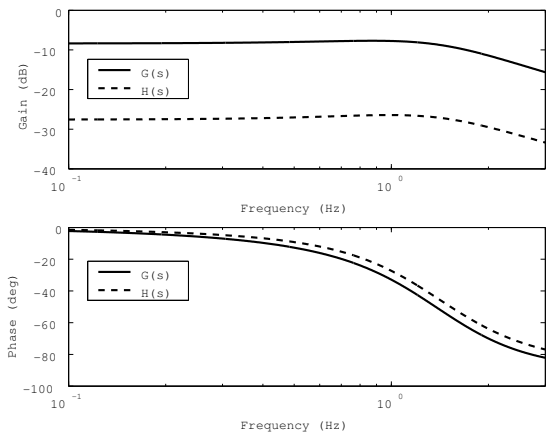

Fig. 8. Bode Diagram of Identified Transfer Functions

X. Evaluation of handling and stability

Evaluation of vehicle handling and stability is done based on the identified transfer functions for steering angle input.

A. Evaluation parameters

In MMC one commonly used method to evaluate vehicle handling and stability is based on 4 representative parameters f_n, ζ, A and ϕ. Here, $f_n = \omega_n/2\pi$, ζ and $A = A_G$ are derived from identified transfer function $G(s)$, and ϕ is the phase delay of lateral acceleration to steering angle input (@1Hz).

Each parameter respectively corresponds to quick response of yaw rate, quick damping of yaw rate, rotational ability and quick response of lateral acceleration, in relation to steering angle input.

[Calculation Method for Phase Delay ϕ]
First we identify the transfer function from steering angle to lateral acceleration using the same method as mentioned in the previous section (from linear approximation the numerator and denominator are both set to second order), then calculate the frequency response to obtain the phase delay.

[4-parameter Calculation Results]
4-parameter values derived from the experiment are as follows: $f_n = 1.42$, $\zeta = 0.665$, $A = 0.382$, $\phi = -74.0$.

B. Improving vehicle handling and stability

Vehicle handling and stability is affected by mass, load distribution, yaw moment of inertia, wheel-base, suspension characteristics, tire cornering power and other factors. Because of limitations in cost and vehicle class, the above may not be possible to change, but by applying DYC handling and stability can be improved. On the other hand, for high performance cars the 4-parameter values are generally large. So when 4-parameter values are plotted on a radar chart like Fig.9, the quadrangle size will become greater for high performance cars[7]. In Fig.9 the dashed line shows COLT EV and the solid line shows a MMC high performance car. Therefore the aim of DYC is to enlarge all of the 4-parameter values. Now ζ and A are large enough compared to the high performance car, whereas f_n and ϕ are obviously small, so in this paper we focus the control objective on enlarging f_n and ϕ.

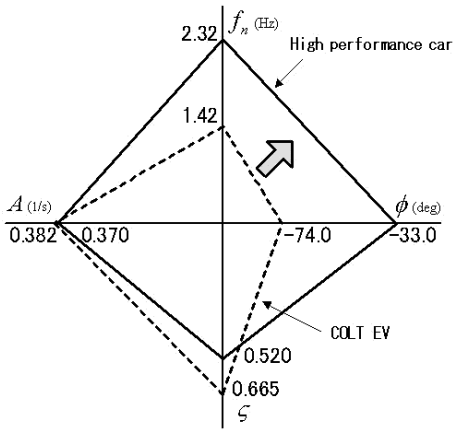

Fig. 9. Radar Chart Comparison of 4 Parameters

XI. DYC and its effect

We will construct a DYC logic based on the identified transfer functions and evaluate the effect through experiments.

A. Target yaw rate

The target yaw rate is the ideal yaw rate response for any steering angle input. When DYC is applied the real yaw rate must trace the target yaw rate. In this paper target yaw rate is given as the output of an ideal transfer function (reference model), and the aim of the control logic is to fit the real vehicle response characteristics to the reference model. This is known as model matching method. In Sec.IX the transfer function $G(s)$ is shown to have the form of Eq.15. Accordingly when making f_n larger to f_n', target yaw rate γ^* and a reference model $F(s)$ are set as follows:

$$\gamma^* \quad = \quad F(s)\theta = \frac{A_G(1+T_G s)}{1+\frac{2\zeta}{\omega_n'}s+\frac{1}{{\omega_n'}^2}s^2}\theta \qquad (16)$$

When f_n value is increased, yaw rate phase delay in high frequency region improves, thus lateral acceleration delay will also be improved. This will be investigated by experiments (Sec.XI-C).

B. DYC logic

For the real yaw rate and target yaw rate to be equal, the following condition must be satisfied.

$$\gamma^* - \gamma \quad = \quad F(s)\theta - \{G(s)\theta + H(s)T_{\rm dif}\} = 0 \qquad (17)$$

From Eq.17 the torque difference required can be calculated, so we use it as a feedforward term. Considering model error and effect of disturbance for real system, we construct the control logic adding a feedback term as shown below.

$$T_{\rm dif} \quad = \quad \frac{F(s)-G(s)}{H(s)}\theta + K_{\rm FB}(s)\{F(s)\theta - \gamma\} \qquad (18)$$

Where $K_{\mathrm{FB}}(s)$ is an appropriate transfer function. The block diagram is shown in Fig.10.

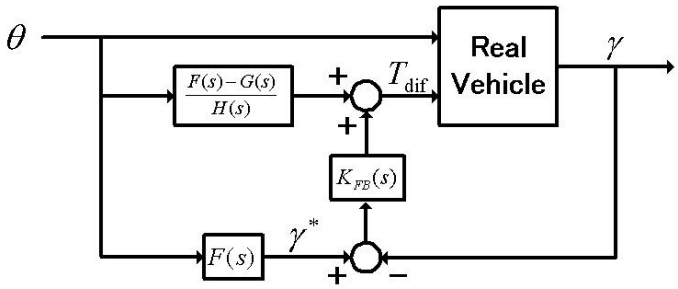

Fig. 10. Block Diagram of DYC Control Logic

C. Experimental evaluation of DYC

Control logic parameters are (i) $\omega_n' = 2\pi f_n \times 1.5$, (ii) $K_{\mathrm{FB}}(s) = 25$ (proportional control). Vehicle speed is set at 80km/h same as in identification experiment (Sec.IX).

[Time domain evaluation]

Steering angle step input is applied to the vehicle. The results are shown in Fig.11 (top is steering angle, middle is motor torque difference control input and bottom is yaw rate output). The yaw rate with DYC (solid line) displays a faster response than the yaw rate without DYC (dashed line), but some modification on control logic or parameters might be needed so that it traces the target yaw rate (dotted line) precisely.

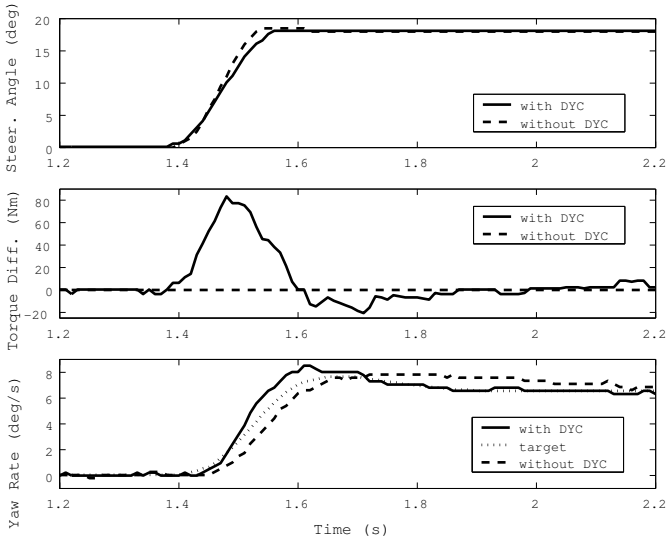

Fig. 11. Time Response of Controlled Yaw Rate

[4 parameter evaluation]

4-parameter values with DYC derived from the identified transfer functions are as follows: $f_n = 1.82$, $\zeta = 0.695$, $A = 0.382$, $\phi = -48.0$. Our control objective to enlarge f_n and ϕ has been achieved. These 4-parameter values are plotted in Fig.12 (with DYC: solid line, without DYC: dashed line). In Sec.X-B it is seen that a vehicle exhibiting superior handling and stability is characterized by large quadrangle. Therefore by observing this radar chart we can quantitatively understand that DYC has improved the vehicle handling and stability.

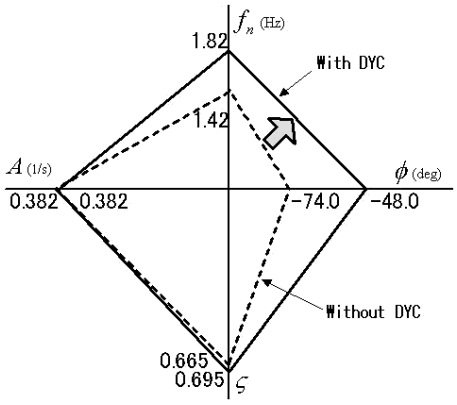

Fig. 12. Radar Chart Comparison of 4 Parameters (with DYC)

XII. Conclusion

In this paper, we proposed control strategies for future motion control to be realized by in-wheel motored electric vehicle. These strategies can be used for motion control of EV especially in the case of tracing the desired yaw rate while minimizing vehicle sideslip. An important method of dynamic distribution control used to resolve the actuator redundancy has also been proposed.

Next, an improvement in vehicle handling and stability resulting from implementing DYC is clearly seen from experiments using the COLT EV test vehicle.

The effect of DYC for dry road and low lateral acceleration region (at linear tire characteristics) has been verified. Therefore we are planning to repeat tests on slippery road and high lateral acceleration conditions.

References

[1] Yoichi Hori, "Future Vehicle driven by Electricity and Control -Research on 4 Wheel Motored 'UOT March II'", *IEEE Transactions on Industrial Electronics*, Vol. 51, No. 5, pp. 954–962, 2004.10

[2] Shin-ichiro Sakai, Hideo Sado and Yoichi Hori, "Motion control in an electric vehicle with 4 independently driven in-wheel motors", *IEEE Trans. on Mechatronics*, Vol. 4, No. 1, pp. 9–16, 1999

[3] Motoki Shino, Masao Nagai, "Yaw-moment control of electric vehicle for improving handling and stability", *JSAE Review*, No. 22, pp. 473–480, 2001.

[4] John A. M. Petersen, Marc Bodson, "Constrained Quadratic Programming Techniques for Control Allocation", *Proceedings of the 42nd IEEE Conference on Decision and Control*, Maui, Hawaii, USA, 2003.12

[5] Ola Harkegard, "Backstepping and Control Allocation with Applications to Flight Control", *Ph.D. Thesis*, Submitted to the Department of Electrical Engineering, Linkoping University, Linkoping, Sweden, 2003.

[6] Road vehicles - Lateral transient response test methods - Open-loop test (JASO Z110)

[7] Tadao Tanaka, Masanori Tani, Hiroo Yuasa, Tetsushi Mimuro, Hiroaki Yoshida, "Active Control Technology For Passenger Car", 22nd *International Congress of FISITA*, Dearborn, USA, No.885105, 1988.9